Flow-Induced Vibration, Bearman (ed.) © 1995 Balkema, Rotterdam. ISBN 90 5410 547 X

Flow-induced chaotic oscillations

J. Mrozowski & J. Awrejcewicz
Technical University of Lodz, Division of Control and Biomechanics, Poland

ABSTRACT: The mathematical model of a rectangular, thin, flat plate submitted to the aerodynamic force action, which consists of three nonlinear partial differential equations, is given. The Galerkin procedure is used to reduce the problem to the consideration of two amplitude equations. Further analysis includes both analytical and numerical techniques leading to the detection of the Hopf bifurcation, and then also of chaotic motion. Some new nonlinear phenomena that have occured in the system under considerations are discussed and illustrated.

1 INTRODUCTION

In this paper we consider the oscillations of a rectangular plate submitted to a constant aerodynamic force action. Generally, nonlinear dynamics of the plates have been analysed by many authors: Bolotin [1963], Brush [1975], Chia [1980], Dowell [1966, 1967, 1975, 1982], Holmes [1977]. However, our attention is concentrated on the investigations of the bifurcation and chaotic oscillations of a rectangular plate caused by aerodynamic force. The first attempt to analyse the bifurcation occurring in the rectangular plate submitted to the action of the aerodynamic forces and external compressive force was made by Holmes [1977]. This type of problem has been analysed also by Bolotin [1963] and recently by Dowell [1966, 1967, 1975, 1982]. Because our attention is focused on the bifurcation phenomena and chaotic motion, we will follow to some extend the approach presented by Dowell, where the direction of the acting airflow and the direction of the external compressive force are parallel to the free supported ends of the plate. This one dimensional model permits an approximate solution in the form of the sinusoidal series with respect to the coordinate x. Dowell's investigation concerns the influence of two essential control parameters, i.e. the velocity of the airflow and the magnitude of the external compressive force on the transition from steady state (equilibrium) to a periodic motion (flutter). Then Dowell has proved numerically the occurrence of chaotic motion by the plate. Contrary to his approach, in our model we have additionally a concentrated mass m_1 placed at the point (x_0,y_0) of the plate. Finally, in our case the direction of the acting aerodynamic force is perpendicular to the freely supported ends of the plate.

Our theoretical approach develops the ideas presented in Awrejcewicz [1989,1991]. After getting the averaged governing ordinary amplitudes differential equations we formulate the Hopf condition analytically and obtain periodic oscillations of the analysed system. Then by varying two control parameters, we analyse two different routes to chaos, transitional and steady state chaotic behaviour.

2 MATHEMATICAL MODEL

We consider a rectangular, long, thin, flat plate of length a, width b ($b<a$) and thickness h, which is small in comparison with its other dimensions. It is assumed that the plate consists of a perfectly homogeneous isotropic material. The concentrated mass m_1 is placed at the point (x_0,y_0) of the plate. The airflow with velocity U acts on the plate in the direction parallel to the y axis. The plate is referred to the rectangular Cartesian coordinates x,y,z, where x and y lie in the middle plane of the plate and z is measured from the midsurface of the plate. We

assume that the plate is subjected to the classical Hooke's law, but the geometrical nonlinearities, which appear as a result of taking into account the rotations of structural elements, play an essential role.

Based on the theory of the virtual work three equilibrium equations in the x,y and z directions are derived.

$$\frac{\partial N_x}{\partial x} + \frac{\partial N_{xy}}{\partial y} = 0 , \tag{2.1a}$$

$$\frac{\partial N_y}{\partial y} + \frac{\partial N_{xy}}{\partial x} = 0 , \tag{2.1b}$$

$$D\frac{\partial^4 w}{\partial x^4} + 2D\frac{\partial^4 w}{\partial x^2 \partial y^2} + D\frac{\partial^4 w}{\partial y^4} - N_x\frac{\partial^2 w}{\partial x^2} - 2N_{xy}\frac{\partial^2 w}{\partial x \partial y} +$$

$$- N_y\frac{\partial^2 w}{\partial y^2} + m\frac{\partial^2 w}{\partial t^2} + m_1\delta(x-x_0, y-y_0)\frac{\partial^2 w}{\partial t^2} +$$

$$+ \frac{\rho U^2}{M}\left(\frac{\partial w}{\partial y} + \frac{1}{U}\frac{\partial w}{\partial t}\right) = 0 , \tag{2.1c}$$

where: N_x, N_y, N_{xy} are the membrane forces per unit length in the rectangular Cartesian coordinates; u,v,w are displacement components in the midsurface in the x,y,z directions, respectively; D is the flexural plate stiffness; m is the plate mass per area; m_1 is the concentrated mass; $\delta(x_0,y_0)$ is the Dirac delta; ρ is the air density; U is the air velocity; M is the Mach number and t denotes time.

The first two equations describe the static equilibrium conditions of a *dxdy* element of the plate along the x and y axes, respectively. The third equation presents the dynamic equilibrium condition along the z axis. The first three terms of the equation (2.1c) can be easily obtained using the classical linear plate theory. Three further terms appear as a result of the consideration of the geometrical nonlinearity. The terms including masses m and m_1 are the inertial terms. The last term describes the aerodynamic force, which consists of two parts: the force generated by the convection velocity $U(\partial w/\partial y)$ and the force generated by the direct velocity $\partial w/\partial t$. The details dealing with the derivation of the formulas of the aerodynamic force can be found in Dowell [1975] and will not be repeated here. It should also be pointed out that this equation plays a fundamental role in further considerations.

The following boundary conditions are taken into account:

for x=0,a:

$$w = M_x = 0 ,$$
$$N_x = N_{xy} = 0 , \tag{2.2a}$$

for y=±b/2:

$$N_y = N_{xy} = 0 . \tag{2.2b}$$

We assume the following solution form

$$w = a_1 w_1 + a_2 w_2 , \tag{2.3a}$$

$$w_1 = \sin(qx) , \quad w_2 = y\sin(qx) , \tag{2.3b}$$

where a_1, a_2 are the amplitudes of the flexural and torsional oscillations, respectively, and $q=n\pi/a$ $(n=1,2,\ldots)$ is the modal number. The torsional oscillation occurs because our plate is long and the direction of the airflow is perpendicular to the free supported edges of the plate.

The approximate expression for the unknown membrane forces is

$$N_x = 0 , \quad N_y = 0 ,$$
$$N_{xy} = a_2^2\frac{Ehq^2}{4(1+\nu)}y\left(\frac{a}{2} - x - \frac{1}{2}q\sin(2qx)\right) . \tag{2.4}$$

Now we use the Galerkin method to reduce the problem to the considerations of the nondimensional ordinary differential equations and the following amplitude equations are obtained:

$$\begin{aligned} \ddot{A}_1 + \beta_1\ddot{A}_2 + \varepsilon\dot{A}_1 + A_1 + \gamma A_2 &= 0 \\ \alpha\ddot{A}_2 + \beta_2\ddot{A}_1 + \varepsilon\dot{A}_2 + A_2 + \eta A_2^3 &= 0 \end{aligned} \tag{2.5}$$

where:

$$A_1 = \frac{a_1}{h} , \quad A_2 = a_2 , \quad \beta = \frac{m_1}{abm} ,$$

$$\alpha = \frac{2+3\beta}{2(1+2\beta)} , \quad \beta_1 = \frac{\beta}{2(h/b)(1+2\beta)} ,$$

$$\beta_2 = \frac{6\beta(h/b)}{(1+2\beta)} , \quad \varepsilon = \frac{\rho U_s}{q^2\sqrt{mD(1+2\beta)}} , \tag{2.5a}$$

$$\gamma = \frac{\rho U^2}{MhDq^4} , \quad \eta = \frac{3(1-\nu)}{2h^2q^2} .$$

The set (2.5) consists of the nonlinear and ordinary autonomous differential equations. The only nonlinear term appears in the second equation of (2.5) and is generated by the membrane force N_{xy}.

3 DETERMINATION OF THE THRESHOLD OF THE PERIODIC OSCILLATIONS

The periodic oscillations appear when with a change of the control parameter a pair of complex conjugate eigenvalues crosses the imaginary axis with the nonzero velocity. This phenomenon is often called as the Hopf bifurcation (Guckenheimer [1986], Huseyin [1983], Iooss [1980], Marsden [1989], Seydel [1988]). The aim of our approach is to find the Hopf condition analytically. First we transform the system of equations (2.5) to the following one:

$$\begin{cases} \dot{x}_1 = x_3 \\ \dot{x}_2 = x_4 \\ \dot{x}_3 = c_{31}x_1 + c_{32}x_2 + c_{33}x_3 + c_{34}x_4 + r_3x_2^3 \\ \dot{x}_4 = c_{41}x_1 + c_{42}x_2 + c_{43}x_3 + c_{44}x_4 + r_4x_2^3 \end{cases} \tag{3.1}$$

where:

$$x_1=A_1\ ,\quad x_2=A_2\ ,\quad x_3=\dot{A}_1\ ,\quad x_4=\dot{A}_2\ ,$$

$$c_{31} = -\frac{\alpha}{\alpha-\beta_1\beta_2} = -\frac{(2+3\beta)(1+2\beta)}{2+7\beta}\ ,$$

$$c_{32} = -\frac{\beta_1-\gamma\alpha}{\alpha-\beta_1\beta_2} = \left[\frac{\beta}{h/b} - \gamma(2+3\beta)\right]\frac{1+2\beta}{2+7\beta}\ ,$$

$$c_{33} = \frac{\varepsilon\alpha}{\alpha-\beta_1\beta_2} = -\frac{\rho U_z(2+3\beta)\sqrt{1+2\beta}}{q^2(2+7\beta)\sqrt{mD}}\ ,$$

$$c_{34} = \frac{\beta_1\varepsilon}{\alpha-\beta_1\beta_2} = \frac{qU_z\beta\sqrt{1+2\beta}}{q^2(2+7\beta)(h/b)\sqrt{mD}}\ ,$$

$$r_3 = \frac{\beta_1\eta}{\alpha-\beta_1\beta_2} = \frac{3}{2}\frac{\beta(1-\nu)}{(h/b)h^2q^2}\frac{1+2\beta}{2+7\beta}\ ,$$

$$c_{41} = \frac{\beta_2}{\alpha-\beta_1\beta_2} = \frac{12\beta(h/b)(1+2\beta)}{2+7\beta}\ ,$$

$$c_{42} = \frac{\beta_2\gamma-1}{\alpha-\beta_1\beta_2} = \frac{[12(h/b)\beta\gamma-4\beta-2](1+2\beta)}{2+7\beta}\ ,$$

$$c_{43} = \frac{\beta_2\varepsilon}{\alpha-\beta_1\beta_2} = \frac{12\beta(h/b)\rho U_z\sqrt{1+2\beta}}{q^2(2+7\beta)\sqrt{mD}}\ ,$$

$$c_{44} = -\frac{\varepsilon}{\alpha-\beta_1\beta_2} = -\frac{2\rho U_z\sqrt{1+2\beta}}{q^2(2+7\beta)\sqrt{mD}}\ ,$$

$$r_4 = -\frac{\eta}{\alpha-\beta_1\beta_2} = -\frac{3(1-\nu)(1+2\beta)^2}{h^2q^2(2+7\beta)}\ . \tag{3.2}$$

We consider the equilibrium point $x_0=\mathbf{0}$. Then, we locally perturb this solution and obtain the linearized set of differential equations, whose Jacobi matrix is given below:

$$\boldsymbol{J}(\mathbf{0}) = \begin{bmatrix} 0 & 0 & 1 & 0 \\ 0 & 0 & 0 & 1 \\ c_{31} & c_{32} & c_{33} & c_{34} \\ c_{41} & c_{42} & c_{43} & c_{44} \end{bmatrix}\ . \tag{3.3}$$

The eigenvalues of the matrix $\boldsymbol{J}$ can be found from the characteristic equation

$$\lambda^4+\alpha_3\lambda^3+\alpha_2\lambda^2+\alpha_1\lambda+\alpha_0 = 0\ , \tag{3.4}$$

where:

$$\begin{aligned} \alpha_3 &= -c_{33}-c_{44} \\ \alpha_2 &= c_{33}c_{44}+c_{33}c_{42}-c_{32}c_{43}-c_{31} \\ \alpha_1 &= c_{33}c_{42}-c_{32}c_{43}-c_{34}c_{43}+c_{31}c_{44}-c_{41}c_{34} \\ \alpha_0 &= c_{31}c_{42}-c_{32}c_{41}\ . \end{aligned} \tag{3.4a}$$

According to the Hopf bifurcation theorem (Marsden [1989]), in the critical point there is one pair of conjugate purely imaginary eigenvalues $\lambda=\pm i\omega$. We take $\lambda=+i\omega$ and substitute it to the characteristic equation (3.4), which leads to

$$\begin{cases} \omega^4-\alpha_2\omega^2+\alpha_0 = 0 \\ -\alpha_3\omega^3+\alpha_1\omega = 0 \end{cases} \tag{3.5}$$

(When we take $\lambda=-i\omega$, we get the same result.)

Eliminating the parameter ω from (3.5), we obtain:

$$\alpha_1^2-\alpha_1\alpha_2\alpha_3+\alpha_0\alpha_3^2 = 0\ , \tag{3.6}$$

with the additional inequality to be fulfilled

$$\alpha_1/\alpha_3>0\ . \tag{3.7}$$

Taking into account the equations (3.4a) we obtain from (3.6) the Hopf condition in the parameter plane γ-β.

In our case we have examined the plate for different values of the ratio a/b=1,3,5,10. We have not found quantitative differences in nonlinear behaviour of the system. The aim of our research is focused on tracking qualitative analysis of bifurcation and chaotic phenomena mainly. Two main results discussed in the paper, i.e. occurrence of the Hopf bifurcation threshold as well as nonlinear phenomena associated with the chaotic scenario are indeed very similar. For this reason we have limited ourselves to present and discuss the result for the ratio a/b=10. We take the following geometrical and physical parameters of the system as fixed: length $a=10$ m, width $b=1$ m, thickness $h=0.005$ m, material density $\varrho_m=7.85\cdot10^3$ kg/m^3, modulus of elasticity $E=2.1\cdot10^{11}$ N/m^2, Poisson's ratio $\nu=0.3$, and we obtain the graphic representation of the equation (3.6), which is shown in Figure 1.

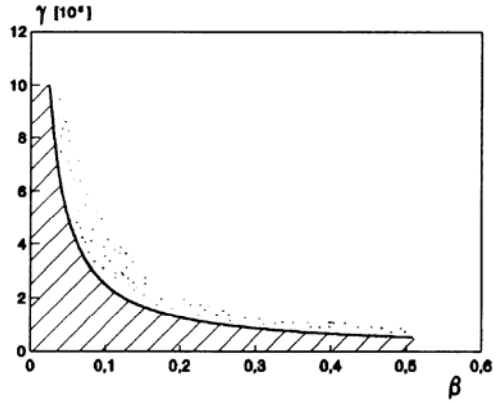

Figure 1. The Hopf bifurcation diagram

The dashed area in this Figure corresponds to the values of parameters, for which the plate is in the stationary steady state (static equilibrium position). After crossing a curve the Hopf bifurcation occurs. In the close neighbourhood over this curve (dotted region) the steady state becomes unstable, and the periodic motion occurs.

4 DYNAMICS OF THE SYSTEM AFTER THE HOPF BIFURCATION

We have found the periodic orbits for the parameters of the system (2.5) in the neighbourhood and upon the bifurcation curve. Now we want to investigate if there are any other attractors or if the found periodic orbits are persistent against the changes of the control parameters.

The analytical methods applied to the investigation of nonlinear behaviour of oscillatory systems usually lead to complicated analytical formulas and generally do not give correct "enough" results. The reason is that only in some rare cases the system of nonlinear equations can be analytically integrated and our system is considered to be a complex one (two degrees of freedom system). We have decided to use only numerical techniques to avoid the occurrence of such potential problems.

Again we use two control parameters β and γ to observe numerically the behaviour of the periodic orbits found earlier.

The analysis has been done for a few arbitrarily chosen rectangular plates with different geometrical and physical properties. All the considered cases have been investigated in a similar way. For the fixed value of the parameter β we increased the parameter γ beginning from the values close to the Hopf bifurcation curve. For each pair of the β and γ values we have observed time histories, phase portraits, Poincaré maps or power spectra. All the mentioned above numerical tools have allowed for the tracing dynamical behaviour of the corresponding analysed system. We have found that for all investigated cases the scenario of the qualitative changes of dynamics is similar.

The numerical analysis has shown, that the periodic motion appears for a broad region of the control parameters plane above the Hopf bifurcation curve. The increase of the γ, which is located close to the Hopf bifurcation point causes the increase of the oscillation amplitude, as well as the increase of the frequencies observed in power spectra (for this purpose Fast Fourier Transformation has been used). There exist values of γ parameter for which first period doubling occurs and a new periodic orbit with a period twice longer in comparison to the previous one is born. The basic periodic orbit becomes unstable. This is the first step of the so-called Feigenbaum scenario, i.e. a cascade of period doubling bifurcation (Reiss [1983], Szemplińska-Stupnicka [1989]). We have observed it numerically using power spectra (see Figures 2a-f).

The sequence of power spectra clearly proves the period doubling scenario. Each next picture contains new frequencies twice smaller in comparison to the previous frequencies. For a certain value of γ the density of the frequency peaks becomes so high, that eventually it is impossible to distinguish among them. This indicates that the system is close to the chaotic motion threshold.

Increasing the parameter γ further above the

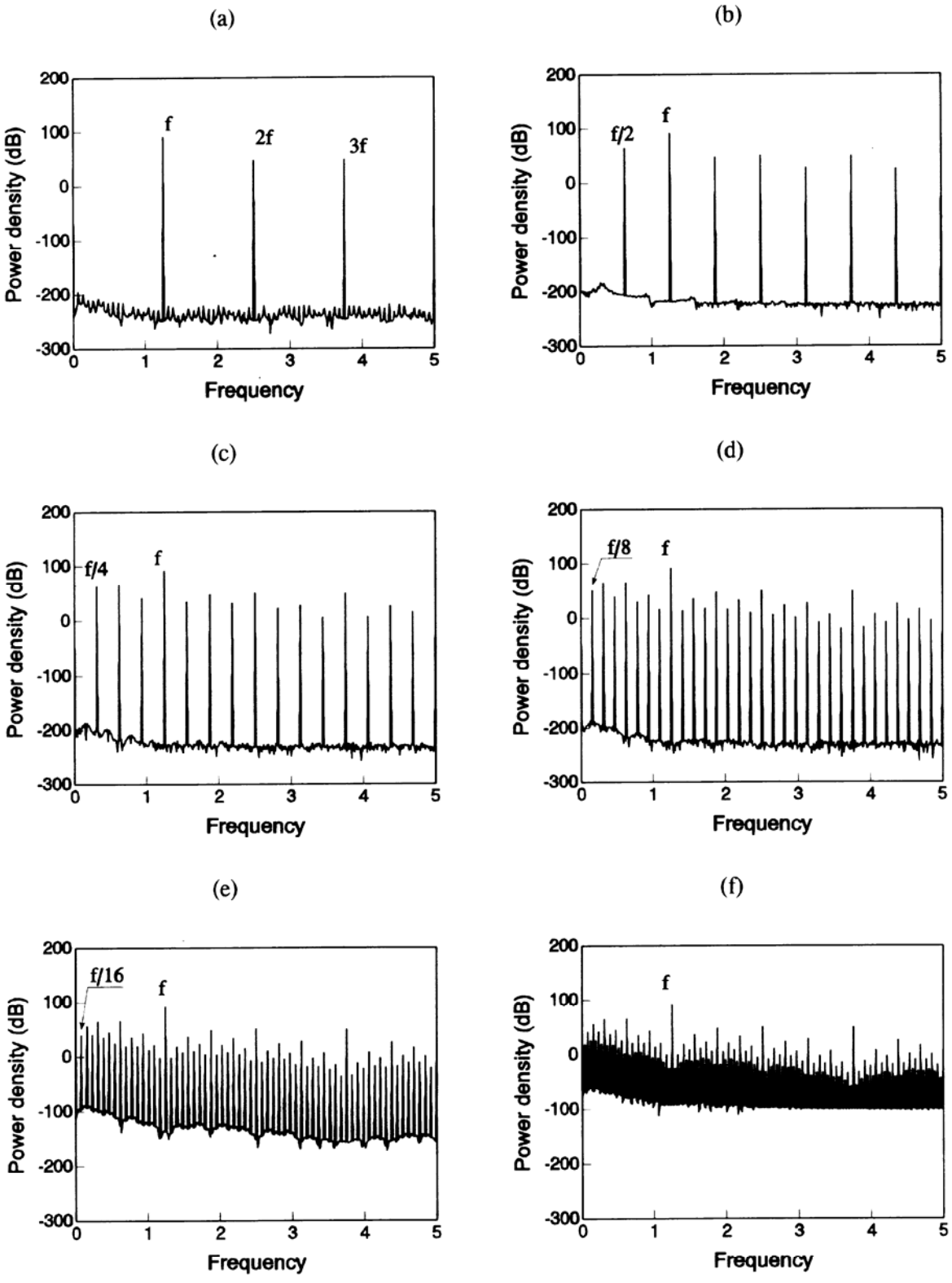

Figure 2. Power spectra illustrating period doubling scenario leading to chaos (β=0.2):
(a) γ=13900, (b) γ=14000, (c) γ=14020, (d) γ=14025, (e) γ=14028, (f) γ=14028.3

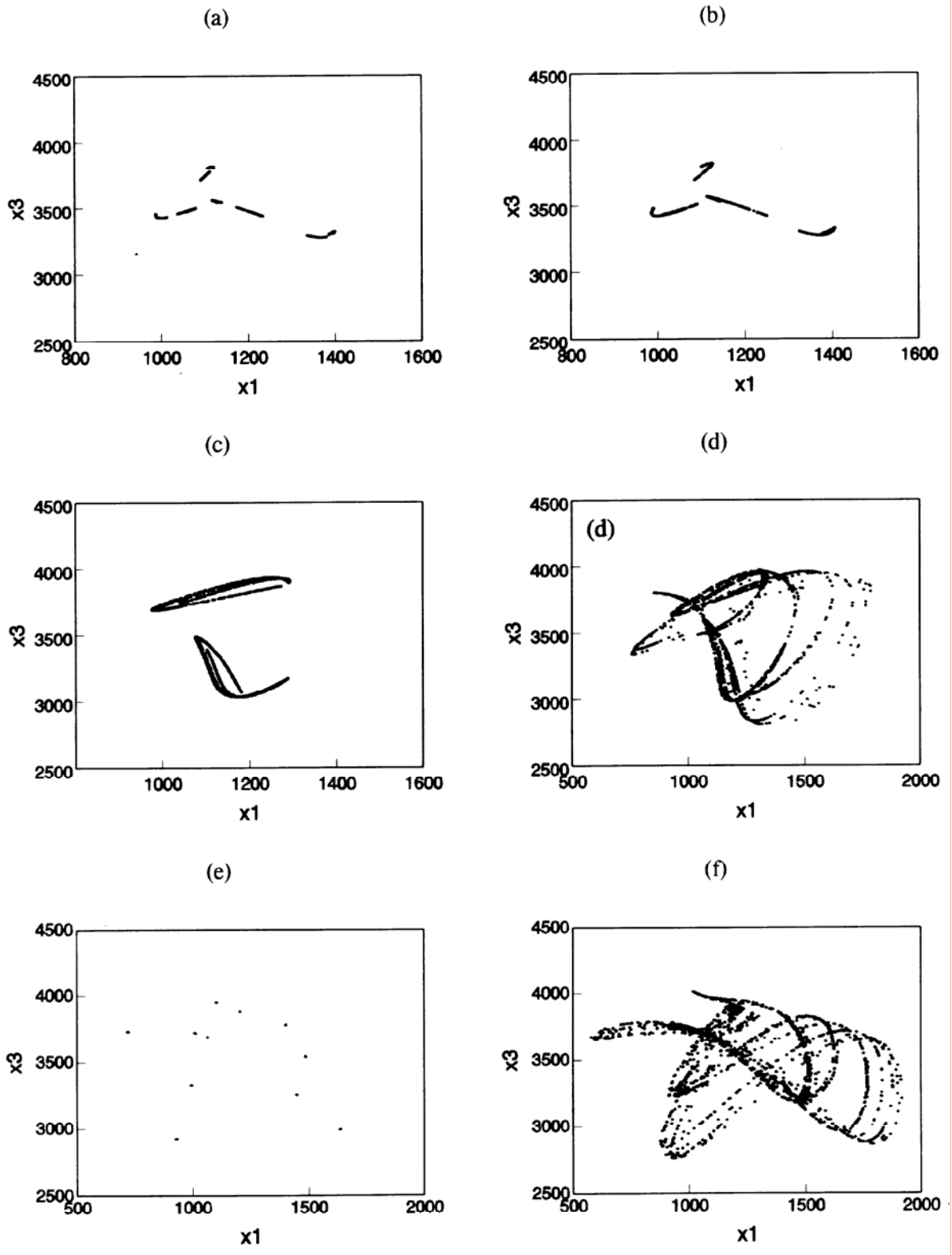

Figure 3. Poincaré maps illustrating the development of chaos with the increase of the control parameter γ (for $\beta=0.2$): (a) $\gamma=14029$, (b) $\gamma=14030$, (c) $\gamma=14035$, (d) $\gamma=14045$, (e) $\gamma=14050$, (f) $\gamma=14055$.

chaotic motion threshold, we have observed a reverse phenomenon, the so called period halving scenario. It is worthy to be emphasized that the vanishing of successive frequency peaks takes place on the broad band power spectrum background. As the result of such a process we finally get one frequency peak plunged in the continuous power spectrum. In Figure 3 the analysis is based on the observation of Poincaré maps. In Figure 3a we can distinguish eight separate parts of a strange chaotic attractor, which correspond to the smallest frequency found in the broad band spectrum, i.e. f/8. This property is observed in each next figure. Two adjacent elements are joined. Finally, we get a fully developed "one element" compact strange attractor. During our numerical simulation we have found that there are some rare intervals of the parameter γ for which the system behaves regularly, the so called periodic windows. The chaotic dynamics of the system is exhibited outside these intervals. This phenomenon is illustrated in Figure 3e.

Increasing the parameter γ further we have found that the scenario beginning from period doubling to full development of chaos repeats a few times.

For a big enough value of γ we have observed another route to chaos. The periodic motion is unpredictably interrupted by sudden jumps of chaos. This phenomenon is called *intermittency* and was introduced first by Manneville-Pomeau during their analysis of one parameter map. The described intermittency scenario is illustrated in Figure 4. As it can be seen in this Figure, in the background of regular motion irregular bursts are clearly visible.

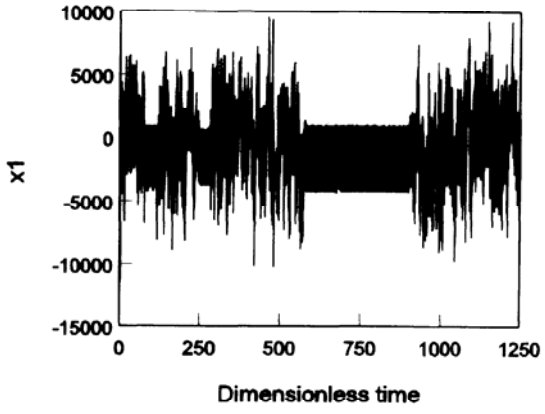

Figure 4. The example of intermittency chaos: $\beta=0.2$, $\gamma=16110$.

5 SUMMARY AND CONCLUDING REMARKS

Our attention has been focused on the nonlinear dynamics of a rectangular plate driven by the aerodynamic force action. We can divide our investigation into two parts. In the first part we emphasize the validity of the technical problems caused by dynamic instability of the rectangular plates, we define much more precisely the object of our investigation, and then we derive the governing equations. The equations are established on the nonlinear thin plate theory. We have taken into account the geometrical nonlinearity due to the rotation of the structure elements. This leads to the three partial differential equations and additionally the boundary conditions have been defined in order to solve the problem. Because the direction of the acting airflow is perpendicular to the free supported edges of the plate and because our plate is long, we search for a particular solution including the expected torsional effects together with the usual bending effects. Then we put the assumed solution to the governing equations set and after applying the Galerkin procedure we finally get the set of two amplitude ordinary differential equations. Thus, as a final result of our investigation, we have reduced the problem to the consideration of two second order ordinary differential equations.

In the second part we have analysed analytically and numerically the obtained earlier set of ordinary differential equations. First we have applied the analytical method in order to define the Hopf conditions. Then we have checked the obtained result using numerical simulation and showing a very good agreement. The key point of our work, however, lies in the investigation of the occurrence of chaotic orbits and the analysis of two independent scenarios leading to it. We have found that above the Hopf bifurcation curve with the increase of one of two control parameters the periodic orbit found earlier (after Hopf bifurcation) becomes unstable, and a new doubled period orbit is born, then it becomes unstable, and a doubling period of new periodic orbit appears and so on. This is the so-called Feigenbaum scenario, which may lead eventually to chaos. During this scenario we have discussed in some detail the development of the strange chaotic attractor, which is accompanied by inverse bifurcation cascade. Additionally, our analysis has been supported by the observation of the Poincaré maps.

During our numerical analysis we have discovered some isolated "periodic windows" plunged in the ocean of chaos.